Hydrogenation of biphenyl and isomeric terphenyls over a Pt-containing catalyst

A. N. Kalenchuk,[a,b] A. E. Koklin,[b] V. I. Bogdan,[a,b] and L. M. Kustov[a,b]*

[a]Department of Chemistry, M. V. Lomonosov Moscow State University, 3 Build., 1 Leninskie Gory, 119992 Moscow, Russian Federation. E-mail: akalenchuk@yandex.ru
[b]N. D. Zelinsky Institute of Organic Chemistry, Russian Academy of Sciences, 47 Leninsky prosp., 119991 Moscow, Russian Federation. Fax: +7 (499) 137 2935

Catalytic hydrogenation of benzene, biphenyl, and *ortho*-, *metha*-, and *para*-isomers of terphenyl over a 3 wt.% Pt/C at 180 °C and 70 atm was studied. The directions of hydrogenation of each substrate were revealed. Relationships between structures of the substrate and hydrogen consumption rates were found. It was shown that hydrogenation rate decreases on going from benzene to terphenyl and with increasing degree of the substrate hydrogenation. Hydrogenation rate of terphenyl isomers decreases in the following order: *p*-terphenyl > > *m*-terphenyl > *o*-terphenyl.

Key words: catalysis, hydrogenation, biphenyl, terphenyl, Pt/C catalyst.

The more stringent limitations set for pollutants during the past 10—15 years and increasing energy efficiency requirements evoke particular interest to hydrogen-based fuel cells. Currently, development of the fuel cell technology attracts the more attention than the hydrogen storage approaches. A modern approache to the hydrogen storage systems involves the use of unsaturated organic compounds, *e.g.*, aromatic and polycyclic aromatic hydrocarbons (PAHs) having hydrogen absorption capacity of >7.0 wt.% (or >65 kg H_2 per 1000 L of substrate). This method is associated with the reversible catalytic hydrogenation—dehydrogenation for hydrogen capture and storage.[1,2] To ensure sustainable hydrogenation/dehydrogenation cycling, high selectivity towards the final products in both direct and reversible reactions should be achieved.

Earlier, by using decalin and perhydroterphenyl as the models we demonstrated that hydrogenation of steric isomers of these compounds follows different pathways thus resulting in the changes of the rates of hydrogen release.[3,4] It is of note that the formation of a large number of intermediates complicates the studies of the features of the transformations of the related compounds. On the other hand, hydrogenation is a prototype of dehydrogenation; therefore, the study of the processes occurring upon saturation of the aromatic analogs of the corresponding polycyclic naphthenes can provide the key information for understanding and planning both these reversible reactions. Kinetics and conditions of the gas phase hydrogenation of benzene and its derivatives over different catalysts are thoroughly studied.[5,6] Liquid-phase hydrogenation of PAHs is less studied; however, dearomatization of PAHs is very important due to their high cancerogenicity and toxicity.[7] It is also should be noted that kinetics of liquid-phase hydrogenation of PAHs over the supported Ni catalysts have been mainly modelled,[8—10] but the nickel catalysts are less efficient for dehydrogenation of the saturated PAH analogs than platinum catalysts.[11,12]

Biphenyl and terphenyl containing, respectively, two and three separate benzene rings are convenient for clarifying the effect of the number of the benzene rings on the behavior of PAHs in hydrogenation reactions. In the present work, we studied liquid-phase hydrogenation of biphenyl and terphenyls over a Pt/C catalyst and compared the obtained results with the data on benzene hydrogenation. The aim of this work is to reveal the relationship between biphenyl and terphenyl structures and their activities in hydrogen consumption.

Experimental

Benzene (Acros Organics, 99.85%), bicyclic aromatic compound biphenyl (Acros Organics, 99%), and tricyclic aromatic compound terphenyl (Santowax-R, a mixture of *ortho*, *meta*, and *para* isomers containing 11.03 wt.% *o*-$C_{18}H_{14}$, 59.22 wt.% *m*-$C_{18}H_{14}$, and 29.75 wt.% *p*-$C_{18}H_{14}$) were used. The main physicochemical properties of the substrates are summarized in Table 1.

Hydrogenation was carried out over a platinum catalyst supported on activated carbon, 3 wt.% Pt/C (Aldrich). The catalyst was loaded into a high pressure PARR-5500 (USA) compact reactor vessel with an inner volume of 600 mL. The

Published in Russian in *Izvestiya Akademii Nauk. Seriya Khimicheskaya,* No. 7, pp. 1208—1212, July, 2017.
1066-5285/17/6607-1208

Table 1. Physicochemical properties of the studied substrates

Substrate	Empirical formula	M.p. / °C	B.p. / °C	Enthalpy of formation (solid) (298.15 K)/kJ mol^{-1} (see Ref. 13)
Benzene	C_6H_6	5—6	80	49.5±0.5
Biphenyl	$C_{12}H_{10}$	69—72	255	100.5±1.5
o-Terphenyl	*o*-$C_{18}H_{14}$	58—59	337	182.5±3.6
m-Terphenyl	*m*-$C_{18}H_{14}$	86—87	379	161.3±3.8
p-Terphenyl	*p*-$C_{18}H_{14}$	212—213	389	158.8±3.4

catalyst was activated for 2 h flowing hydrogen (30 mL min^{-1}) at 305 °C. After cooling to ambient temperature, the reactor was charged with the substrate under nitrogen flow and flashed with nitrogen. Hydrogenation was performed at 180 °C and pressure of 70 atm using mechanical stirring of the reaction mixture at 600 rpm.

The samples were taken at certain time intervals and the content of the products of hydrogenation were analyzed using a KristaLyuks-4000M chromatograph (Russia) equipped with a ZB-5 (Zebron, USA) and TR-FFAP (Thermo Scientific, USA) capillary columns and a flame ionization detector and using a FOCUS DSQ II (Thermo Fisher Scientific, USA) GC/MS system equipped with a TR-5MS (Thermo, USA) capillary column. Conversion of the substrates (X) and selectivity (S) on the products of hydrogenation and dehydrogenation were calculated as follows:

$$X = (c_0 - c)/c_0 \cdot 100\%;$$

$$S = \Sigma c(i)/\Sigma c(k) \cdot 100\%,$$

where c_0 and c are the initial and final concentrations of the starting substrate, respectively, $\Sigma c(i)$ and $\Sigma c(k)$ are the sums of the concentrations of single products and all products, respectively.

Results and Discussion

Hydrogenation of biphenyl is shown on Scheme 1.

Scheme 1

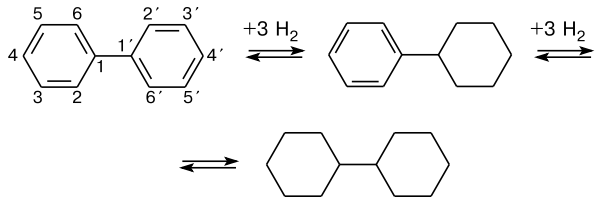

The final product of the biphenyl hydrogenation is bicyclohexyl ($C_{12}H_{22}$). The reaction proceeds *via* intermediate cyclohexylbenzene ($C_{12}H_{16}$).

The results of hydrogenation of biphenyl and benzene at 180 °C and 70 atm are given on Fig. 1. In 20 min after the start, 99.95% conversion of benzene was achieved

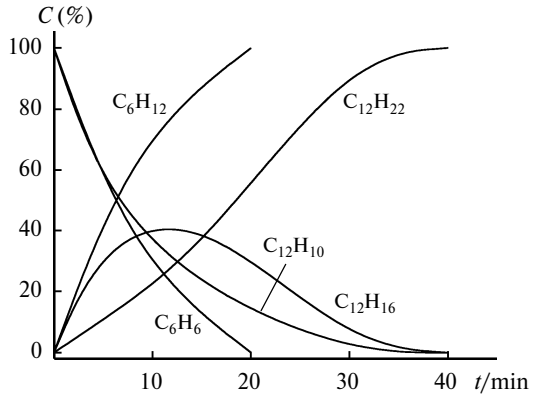

Fig. 1. Concentrations of the products of hydrogenation of benzene and biphenyl *vs.* reaction time (t).

with 70% conversion observed within 8 min. As high as 70% of biphenyl was converted into cyclohexabenzene within 12 min. Under the selected hydrogenation conditions, the conversion of biphenyl into bicyclohexyl equal of 99.5% with 99.9% selectivity was achieved 40 min after the reaction onset. The only intermediate product of biphenyl hydrogenation was cyclohexylbenzene, no other liquid products were detected.

The benzene residue forming the biphenyl molecule is a perfectly regular hexagon with hydrogen at each corner with all external H—C—C and internal C—C—C angles being equal to 120° and the C—C bond lengths being 1.397 Å (0.139 nm). The electron density in benzene (six π electrons) is evenly distributed over the ring providing the additional stability to the structure. The resonance stabilization energy of benzene is higher than the arithmetic mean of the energies of formations of single and double bonds (151 kJ mol^{-1}).[14] According to Balandin´s multiplet theory, benzene hydrogenation follows the sextet mechanism involving interaction of all benzene bonds with one metal atom at the catalyst surface.[15]

Two benzene rings of biphenyl linked by the single C(1)—C(1´) bond are relatively independent.[16] The resonance stabilization energy of biphenyl is 330 kJ mol^{-1}, which is higher than the total stabilization energies of two benzene molecules.[14] Lengths of the C—C ring bonds are nearly the same as those of benzene but the interaction between the rings causes the decrease in the bond angle at the substituted carbon atom up to 117.9° and elongation of the C(1)—C(1´) bond up to 1.48 Å.[17] In the solid state, the biphenyl molecule is planar but in the gas phase the twist angle between the rings is about 45°.[11,18]

Under liquid-phase hydrogenation conditions, the interactions between two benzene rings of biphenyl cause torsional vibrations violating coplanarity of the rings. This, in turn, affects the biphenyl hydrogenation rate. A comparison of the slopes of the product concentration *vs.* time plots (see Fig. 1) indicates that the hydrogenation rate of biphenyl to cyclohexylbenzene is lower than

the rate of the transformation of benzene into cyclohexene. Plots describing further hydrogenation of intermediates to bicyclohexyl and cyclohexane have nearly the same slopes.

Similarly to biphenyl, terphenyl can be regarded as a central benzene ring substituted with two phenyl groups. Terphenyl has three isomers (*ortho*, *meta*, and *para*); their structural formulas are given below (**A**, **B**, and **C**, respectively).

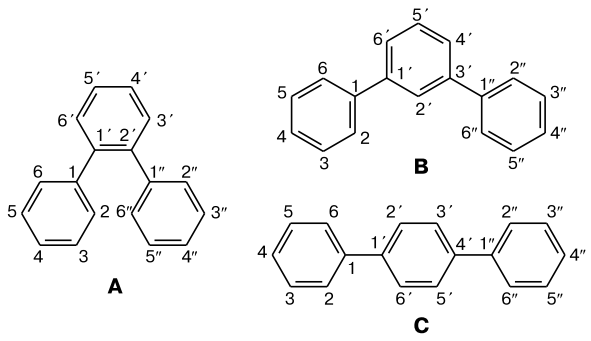

Hydrogenation of terphenyl isomers proceeds as shown on Scheme 2.

Scheme 2

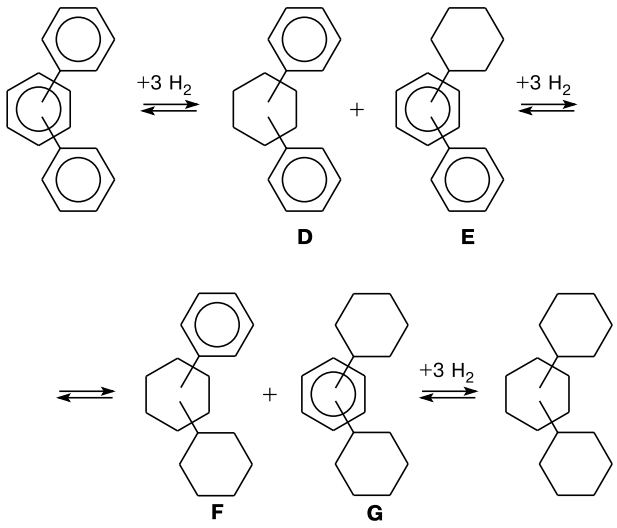

As compared with hydrogenation of biphenyl, terphenyl produces more intermediates. Thus, upon hydrogenation of terphenyl diphenylcyclohexane (**D**), cyclohexylbiphenyl (**E**), phenylbi(cyclohexane) (**F**), and dicyclohexylbenzene (**G**) can be formed. The final products of hydrogenation of *ortho*-, *meta*-, and *para*-terphenyls are perhydro-*o*-terphenyl, -*m*-terphenyl, and -*p*-terphenyl, respectively, each having two sterical isomers.

Results of hydrogenation of a mixture of *o*-, *m*-, and *p*-terphenyls are given on Fig. 2. Hydrogenation of terphenyl isomers gives a mixture containing 12.53 wt.% *o*-$C_{18}H_{32}$, 61.41 wt.% *m*-$C_{18}H_{32}$, and 27.06 wt.% *p*-$C_{18}H_{32}$.

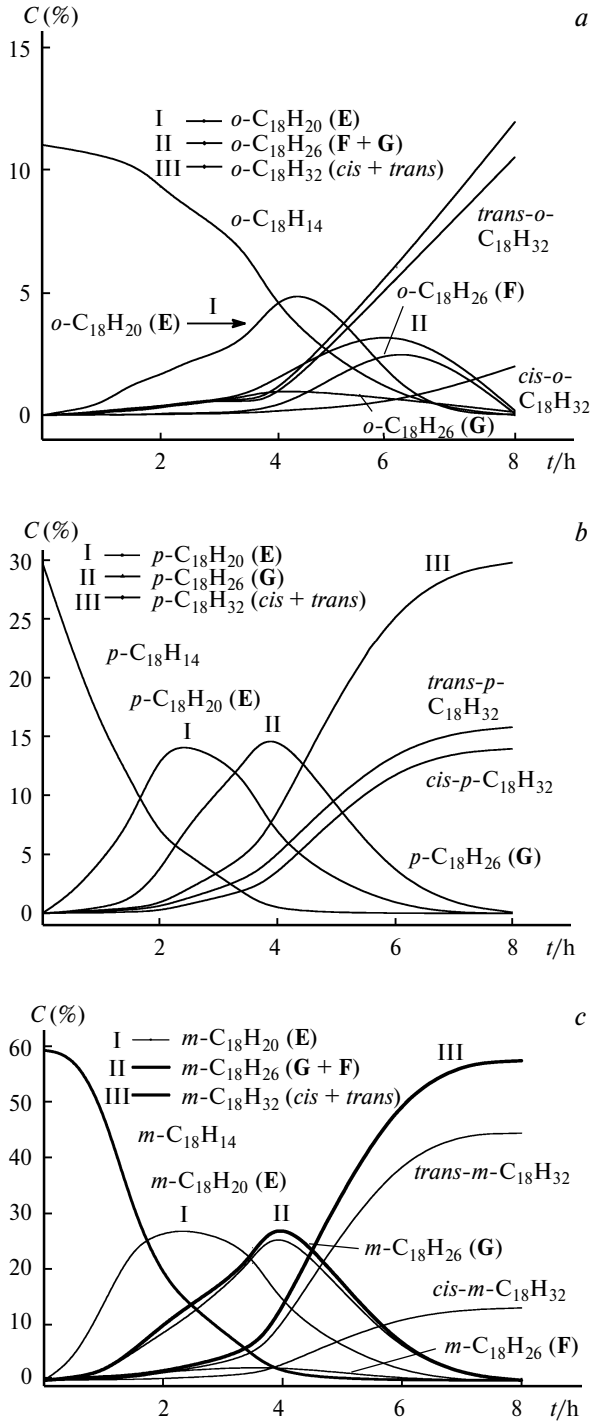

Fig. 2. Concentrations of *o*- (*a*), *p*- (*b*), and *m*-terphenyl (*c*) and products of their hydrogenation *vs.* reaction time.

All products were formally divided onto three groups according to the degree of saturation of the benzene rings. The first group (I, $C_{18}H_{20}$) includes compounds **D** and **E** with one cyclohexane ring; compounds **F** and **G** with two cyclohexane rings were placed in the second group (II, $C_{18}H_{26}$); and the third group of compounds (III, $C_{18}H_{32}$) combines *cis* and *trans* isomers of terphenyl.

The terphenyl molecule is characterized by steric strain between phenyl groups, which differently affects the torsional vibrations in *ortho*-, *meta*-, and *para*-isomers. *o*-Terphenyl was found to be the most distorted; the minimal distortions of the terphenyl isomers were observed in the gas phase.[13] The bond lengths in *o*-terphenyl are identical to those in biphenyl; but the dihedral angles formed by the planes of the central ring and the peripheral rings measured for solid *o*-terphenyl are significantly different from biphenyl (42° and 62°). In the gas phase, both dihedral angles are 53°. The bond angles at the corresponding substituted carbon atoms of *o*-terphenyl in the solid state are 123.6° and 123.0° whereas in the gas phase they are 122.9°.[19,20]

A plot of the concentrations of *o*-terphenyl and the hydrogenation products *vs.* reaction time is shown on Fig. 2, *a*. It is seen that the hydrogenation products appear only 4 h after the reaction onset. Apparently, this delay can be attributed to the delay in the hydrogenation initiation due to the steric hindrance in the *o*-terphenyl molecule. In the course of hydrogenation, as the degree of hydrogenation increases the intramolecular forces between the rings become weaker thus progressively accelerating hydrogenation of the second and the third benzene rings. The main intermediates formed during hydrogenation of *o*-terphenyl are cyclohexylbiphenyl (**E**) and dicyclohexylbenzene (**G**). Phenylbi(cyclohexane) (**F**) is formed in noticeably less amounts and only traces of dicyclohexylbenzene (**G**) were detected. During experiment, 99.5% conversion of *o*-terphenyl was reached within 8 h. Selectivity on perhydro-*o*-terphenyl was 99%.

Three benzene rings of *p*-terphenyl are located along 1,4-axis, therefore, the structure of this terphenyl isomer most closely resembles the structure of biphenyl. In the gas phase, the angles of twisting vibrations of the central and terminal rings of the terphenyl molecules are 42° and 43°, respectively. These values are close to those of biphenyl and, similarly, do not affect the bond lengths and bond angles. In the solid state, the *p*-terphenyl molecule is twisted in contrast to biphenyl. The effect of two terminal phenyl rings of *p*-terphenyl causes the twist of the central ring by ±20° relative to the molecular axis.[13,21] It is also of note that structures of the molecules of *p*- and *o*-terphenyls are significantly different.

Figure 2, *b* shows that the kinetic curves of the hydrogenation of *p*- and *o*-terphenyls have different patterns. Hydrogenation of *p*-terphenyl gives only cyclohexylbiphenyl (**E**) and dicyclohexylbenzene (**G**) as intermediates. A comparison of the slopes of the curves indicates relatively equal rates of hydrogenation of the rings. *p*-Terphenyl hydrogenates noticeably faster than *o*-terphenyl. Thus, under identical hydrogenation conditions 99.5% conversion of *p*-terphenyl was reached within 5 h after the start of the reaction. Selectivity of the reaction on perhydro-*p*-terphenyl was 99.6%.

In terms of the mutual orientation of the benzene rings, the *m*-terphenyl structure is "intermediate" between *o*- and *p*-terphenyls. In the gas phase, the dihedral angles between the central and terminal rings caused by the twisting vibrations in the *m*-terphenyl molecule are smaller than that of *p*-terphenyl and equal to 35° and 38°, respectively. A comparison of the structures of the terphenyl isomers indicates that the isomer with the most perfect planarity is *m*-terphenyl.[13] The intermediates formed upon hydrogenation of *m*-terphenyl are mainly cyclohexylbiphenyl (**E**), phenylbi(cyclohexane) (**F**) and dicyclohexylbenzene (**G**) and small amounts of phenylbi(cyclohexane) (**F**) were also detected. Comparing the slopes of the plots of the product concentrations against the reaction time (Figs 2, *a*—*c*), it can be recognized that the rate of hydrogenation of the first ring of *m*-terphenyl is substantially higher than that of *o*-terphenyl and lower than that of *p*-terphenyl. Hydrogenation rates of the second and the third rings of *m*-terphenyl are lower although these values are close to the hydrogenation rates of the second and third rings of *p*-terphenyl. Under the described conditions, 99.5% conversion of *m*-terphenyl was achieved within 6 h after the reaction onset. Selectivity on perhydro-*m*-terphenyl was 99.9%.

Comparing the data given on Figs 2, *a*—*c*, it can be concluded that the terminal benzene rings of each of three isomers are hydrogenated first to produce initially cyclohexylbiphenyl (**E**) and then dicyclohexylbenzene (**G**). Highly distorted geometry of the formed species provides the access to the central benzene rings and phenylbi(cyclohexane) (**F**) and diphenylcyclohexane (**D**) are formed. As a result, hydrogenation curves of *m*-terphenyl and especially *o*-terpnehyl show wider peaks of compounds of groups I and II as compared with *p*-terphenyl.

Based on the obtained experimental data, the reactivity of the studied substrates towards hydrogenation (measure from the time required to reach 70% conversion) increases in the following order: benzene < biphenyl << << *p*-terphenyl < *m*-terphenyl < *o*-terphenyl. During adsorption, the hydrogenated molecule efficiently interacts with the catalyst, which changes the states of both the adsorbed molecule and the active catalyst surface. The DFT calculation revealed that the adsorption energy ($\Delta E°_{ads}$, eV) of benzene on the Pt(111) face can be well approximated by the parabolic equation[22]

$$E°_{ads} = -0.90 + 2.23\Delta x^2 + 1.94\Delta y^2 + 0.13\Delta x\Delta y,$$

where D*x* and D*y* are the distortion parameters of geometrical sizes of the adsorbed molecule and the metal surface upon substrate—catalyst interaction. The adsorption energy of benzene on the Pt(111) atom in the optimal configuration is −0.90 eV and decreases with increasing geometric distortion. For the polycyclic molecules, $E°_{ads}$

is an additive value reflecting the changes of the structure of each benzene ring constructing the PAH molecule and the surface geometry. With increasing number of the benzene ring in the hydrogenated substrate, the substrate adsorption energy increases; however, according to the above equation for E°_{ads} this increase is not linear, which correlates with the order of the substrate reactivity.

The enthalpy of the reaction can serve as an objective quantitative estimate of the difference of the reactivity of the terphenyl isomers to hydrogenation. Since the stoichiometry of the reaction is the same for all three terphenyl isomers, the differences in the heat effects are mainly predetermined by the standard molar enthalpies of formation of the starting terphenyl isomers and reflect the structural differences between isomers. From Table 1, it is clearly seen that the standard molar enthalpies of formation of *p*- and *m*-terphenyls are close to each other but noticeably different from the value known for *o*-terphenyl. A comparison of the thermodynamic values with the experimental data indicates that the enthalpies of formation simbatically increase with increasing intramolecular interaction between benzene rings of all three isomers.

In summary, the directions of hydrogenation of all studied substrates until formation of completely saturated products were experimentally investigated. For the studied substrates, the relationships reflecting the structural effects on activity in hydrogen consumption were determined. It was found that the rate of hydrogenation decreases on going from benzene to terphenyl and with increasing the degree of substrate hydrogenation. The rate of hydrogenation of the terphenyl isomers decreases in the order *p*-terphenyl > *m*-terphenyl > *o*-terphenyl. No cracking products were found in all experiments when examining analytical samples. This is due apparently to the use of activated carbon support lacking acidic centers on the surface. The revealed relationship between the structures of the studied substrates and their reactivity towards hydrogenation can be of use in designing the efficient catalyst for hydrogenation.

This work was financially supported by the Russian Science Foundation (Project No. 14-50-00126).

References

1. J. S. Sung, Y. Choo Ko, T. H. Kim, A. L. Tarasov, O. P. Tkachenko, L. M. Kustov, *Int. J. Hydrogen Energy*, 2008, **33**, 2721.
2. US Pat. 7101530; http://www.patentscope.wipo.int US2004014034.
3. A. N. Kalenchuk, D. N. Smetneva, V. I. Bogdan, L. M. Kustov, *Russ. Chem. Bull.*, 2015, **64**, 2642.
4. A. N. Kalenchuk, V. I. Bogdan, S. E. Bogorodskii, L. M. Kustov, *Kinet. Catal.*, 2016, **57**, 219.
5. S. Smeds, D. Murzin, T. Salmi, *React. Kinet. Catal. Lett.*, 1998, **63**, 47.
6. B. H. Cooper, B. B. L. Donnis, *Appl. Catal. A*, 1996, **137**, 203.
7. A. Stanislaus, B. H. Cooper, *Catal. Rev.-Sci. Eng.*, 1994, **36**, 75.
8. S. Toppinen, T.-K. Rantakyla, T. Salmi, J. Aittamaa, *Ind. Eng. Chem. Res.*, 1996, **35**, 1824**.**
9. D. Yu. Murzin, N. D. Sokolova, N. V. Kul´kova, M. I. Temkin, *Kinet. Katal.*, 1989, **30**, 1352.
10. L. P. Lindfors, T. Salmi, *Ind. Eng. Chem. Res.*, 1993, **32**, 34.
11. P. Castano, D. Van Herk, M. T. Kreutzer, J. A. Moulijn, M. Makkee, *Appl. Catal.*, *B*, 2009, **88**, 213.
12. A. N. Kalenchuk, V. I. Bogdan, L. M. Kustov, *Catal. Ind.*, 2015, **7**, 60.
13. M. A. V. R. da Silva, L. M. Santos, L. M. S. S. Lima, *J. Chem. Thermodynamics*, 2008, **40**, 375.
14. S. Nishimura, *Handbook of Heterogeneous Catalytic Hydrogenation for Organic Synthesis*, John Willey and Sons, New York, 2001, 737 pp.
15. A. A. Balandin, *Multipletnaya teoriya kataliza*, Ch. 1, *Structurnye fakroty v katalize* [*"Multiplet" Theory of Catalysis*, Part 1, *Structural Effects in Catalysis*], Izd-vo MGU, Moscow, 1963.
16. D. B. Berezin, B. D. Berezin, *Kurs sovremennoi organicheskoi khimii* [*Course of Modern Organic Chemistry*], Vysshaya Shkola, Moscow, 1999, 756 pp.
17. Z. V. Zvonkova, *Russ. Chem. Rev.*, 1977, **46**, 479.
18. G. P. Charbonneau, Y. Delugeard, *Acta. Crystallogr.*, 1976, **B32**, 1420.
19. M. P. Eastwood, T. Chitrat, J. M. Jumper, K. Palmo, A. C. Pant, D. E. Shaw, *J. Phys. Chem. B*, 2013, **117**, 12898.
20. G. M. Brown, H. A. Levy, *Acta Crystallogr.*, 1979, **B35**, 785.
21. J. L. Baudour, Y. Delugeard, H. Caileau, *Acta Crystallogr.*, 1976, **B32**, 150.
22. C. Morin, D. Simon, P. Sautet, *J. Phys. Chem. B*, 2004, **108**, 12084.

Received December 21, 2016;
in revised form April 6, 2017